



HAL
open science

Legionella pneumophila sg1-sensing signal enhancement using a novel electrochemical immunosensor in dynamic detection mode

Ahlem Laribi, Séverine Allegra, Mina Souiri, Ridha Mzoughi, Ali Othmane, Françoise Girardot

► To cite this version:

Ahlem Laribi, Séverine Allegra, Mina Souiri, Ridha Mzoughi, Ali Othmane, et al.. Legionella pneumophila sg1-sensing signal enhancement using a novel electrochemical immunosensor in dynamic detection mode. *Talanta*, 2020, 215, pp.120904. 10.1016/j.talanta.2020.120904 . hal-02512942

HAL Id: hal-02512942

<https://hal.science/hal-02512942>

Submitted on 20 May 2022

HAL is a multi-disciplinary open access archive for the deposit and dissemination of scientific research documents, whether they are published or not. The documents may come from teaching and research institutions in France or abroad, or from public or private research centers.

L'archive ouverte pluridisciplinaire **HAL**, est destinée au dépôt et à la diffusion de documents scientifiques de niveau recherche, publiés ou non, émanant des établissements d'enseignement et de recherche français ou étrangers, des laboratoires publics ou privés.



Distributed under a Creative Commons Attribution - NonCommercial 4.0 International License

1 ***Legionella pneumophila* sg1-sensing signal enhancement using a novel**
2 **electrochemical immunosensor in dynamic detection mode**

3
4 **Ahlem Laribi^{1,2*}, Séverine Allegra¹, Mina Souiri², Ridha Mzoughi³, Ali Othmane², and Françoise**
5 **Girardot¹**

6 ¹ *Environments, Territories, Societies (EVS) Lab, Mixed Research Unit (Jean Monnet University -*
7 *French National Centre for Scientific Research) 5600, University of Lyon, F42023, France;*

8 ² *Laboratory of advanced materials and interfaces, Faculty of Medicine, University of Monastir - 5019*
9 *Monastir, Tunisia;* ³ *Regional Laboratory of Hygiene, University Hospital Farhat Hached, 4000 Sousse,*
10 *Tunisia and Laboratory of analysis treatment and valorization of pollutants and products, Faculty of*
11 *Pharmacy, 5000 Monastir, Tunisia*

12
13 *Corresponding author

14 A. LARIBI

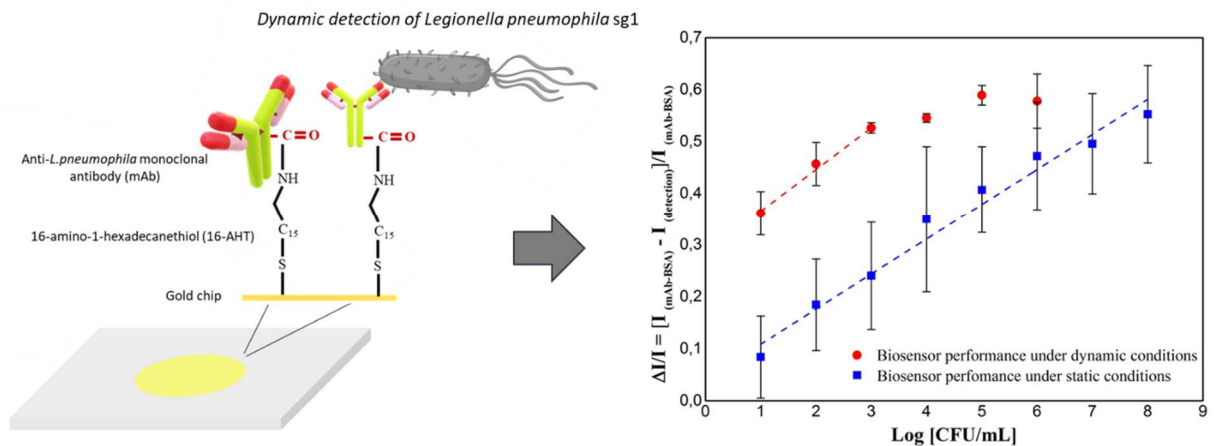
15 Tel: +33 6 46 37 25 16

16 e-mail: ahlem.laribi@etu.univ-st-etienne.fr

17
18 **Abstract**

19 This work presents a comparison between static and dynamic modes of biosensing using a
20 novel microfluidic assay for continuous and quantitative detection of *Legionella pneumophila*
21 sg1 in artificial water samples. A self-assembled monolayer of 16-amino-1-hexadecanethiol
22 (16-AHT) was covalently linked to a gold substrate, and the resulting modified surface was
23 used to immobilize an anti-*Legionella pneumophila* monoclonal antibody (mAb). The
24 modified surfaces formed during the biosensor functionalization steps were characterized
25 using electrochemical measurements and microscopic imaging techniques. Under static
26 conditions, the biosensor exhibited a wide linear response range from 10 to 10⁸ CFU/mL and
27 a detection limit of 10 CFU/mL. Using a microfluidic system, the biosensor responses
28 exhibited a linear relationship for low bacterial concentrations ranging from 10 to 10³
29 CFU/mL under dynamic conditions **and an enhancement of sensing signals by a factor of 4.5**
30 compared to the sensing signals obtained under static conditions with the same biosensor for
31 the detection of *Legionella* cells in artificially contaminated samples.

36 Graphical Abstract



37

38

39 **Keywords.** *Legionella pneumophila*, Electrochemical Detection, Microfluidic Device,
40 Immunosensor

41

42 1. Introduction

43 *Legionella pneumophila* is the main vector of Legionnaires' disease, a type of pneumonia that
44 can be fatal in humans. Indeed, inhalation of contaminated aerosols can cause bilateral
45 pneumonia (Sharma et al., 2017). It has been reported that 9% of domestic cases are fatal
46 (Dooling et al., 2015), reaching between 25 to 48% for nosocomial cases in the USA (Soda et
47 al., 2017). In France, there was a 75% increase in the number of recorded incidences in 2018
48 compared to the previous year (Campese, 2018).

49 *Legionella* bacteria are found in natural aquatic environments and wet soils (Borella et al.,
50 2005). They are known to colonize artificial human-made aquatic ecosystems such as hot
51 water distribution systems, air conditioning systems, and air-cooling towers, thereby giving
52 rise to severe outbreaks of pneumonia (Beer et al., 2015; Mobed et al., 2019a). Approximately
53 28 sources of sporadic cases involving potable water, hot springs, humidifiers, water
54 fountains, and medical respiratory equipment have been identified (Orkis et al., 2018).
55 Therefore, any water system that generates aerosols from water should be considered at-risk
56 (Baldovin et al., 2018; Walker, 2018). For this reason, effective monitoring of water systems
57 is critical. However, current standardized detection and enumeration methods (ISO 11731 and
58 AFNOR T90 431 for cultures and ISO 12869 and AFNOR T90 471 for quantitative PCR)
59 suffer from limitations that hinder proper and timely diagnosis (Mobed et al., 2019a).

60 Analysis by culture takes up to 10 days and the recovery of *Legionella* is not optimal due to
61 the acid treatment and concentration stage (Delgado-Viscogliosi et al., 2005). Viable but

62 nonculturable cells (VBNC), which are compromised cells characterized by a loss of
63 culturability, are not detected using cultures (Kirschner, 2016), whereas it has been
64 demonstrated that they are nonetheless still able to infect amoebae and human macrophages
65 (Alleron et al., 2013; Dietersdorfer et al., 2018). Several studies have demonstrated that
66 VBNC forms are systematically present in potable water sources due to the presence of
67 disinfection products and their low levels of nutrients (Chang et al., 2007; Dietersdorfer et al.,
68 2018).

69 Quantitative PCR (qPCR) is fast and easy to implement. However, it is limited by its inability
70 to discriminate between dead and live cells, not to mention the need for specialized
71 knowledge and experience to operate the equipment.

72 Furthermore, both techniques require harvesting of water samples and further lab-based
73 analyses.

74 Contaminated water systems are mainly disinfected using chlorine or heat treatment by
75 exposure to high temperatures (70 °C for 30 min). It has been shown that up to 25% of
76 *Legionella* bacteria can survive after such a heat treatment, and they are able to regrow after a
77 few months (Allegra et al., 2011). In light of the reasons outlined above, there is hence a clear
78 need to develop fast, sensitive, portable, and easy-to-use devices to achieve continuous
79 monitoring of *Legionella* that can be applied directly to the water system.

80 Biosensors are considered to be a valuable alternative in this field. However, despite their
81 remarkable sensitivity and biological compatibility, only a small number of practical studies
82 have investigated the use of immunosensors to address this issue.

83 In this context, an optical fibre sensor based on surface plasmon resonance has been reported
84 to provide a limit of detection of approximately 10 CFU/mL (Lin et al., 2007). A similar
85 sensitivity can be obtained using an electrochemical impedance spectroscopy immunosensor
86 (Sboui et al., 2015), and this LOD is considered to be the lowest detected concentration. For
87 instance, Li et al. (Li et al., 2012) and Lei et al. (Lei and Leung, 2012) reached LOD values
88 of 10^2 Cells/mL and 10^5 CFU/mL, respectively, using an impedimetric immunosensor to
89 detect *Legionella pneumophila*. Using an amperometric magnetic immunoassay assay for
90 *Legionella pneumophila* detection, Martini et al. reported a LOD of 10^4 CFU/mL, with the
91 possibility of detecting *Legionella* cells at 10 CFU/mL after a preconcentration step (Martín et
92 al., 2015).

93 Using surface plasmon resonance technology for *Legionella pneumophila* detection, Enrico et
94 al. (Enrico et al., 2013) and Foudeh et al. (Foudeh et al., 2015) reported LOD values of $\sim 10^4$
95 CFU/mL. More recently, Aziziyan et al. have used the negative zeta potential, enhanced by

96 decorating *Legionella pneumophila* with negatively charged sodium dodecyl sulphate
97 molecules, to achieve a detection limit of 10^3 CFU/mL (Aziziyan et al., 2020). Despite their
98 high sensitivities, these methods require specific equipment, as well as the necessary skills
99 and expertise to properly interpret the sensing data. By using genosensors, which allow the
100 detection of a specific DNA sequence, several authors have been able to achieve very low
101 quantification limits of 10^{-21} M (Mobed et al., 2019b) and 10^{-14} M (Rai et al., 2012).
102 Nevertheless, despite their high sensitivities, genosensors cannot be used to detect and
103 quantify live bacterial cells in water samples.

104 In light of these various reasons, in this study, we investigated a new version of a microfluidic
105 immunosensor based on a combination of biosensor technology for *Legionella* detection and
106 microfluidic systems.

107 **2. Experimental**

108 **2.1. Chemicals and reagents**

109 Phosphate-buffered saline (PBS) (0.01 M, pH 7.4), sulphuric acid (95-97%), bovine serum
110 albumin (BSA, $\geq 96\%$), hydrogen peroxide solution (H_2O_2 , 30%), acetone, N-(3-
111 Dimethylaminopropyl)-N'-ethylcarbodiimide hydrochloride (EDC), N-Hydroxysuccinimide
112 (NHS), and 16-Amino-1-hexadecanethiol hydrochloride (16-AHT) were purchased from
113 Sigma-Aldrich.

114 BupH™ MES Buffered Saline Packs (MES) were purchased from Thermo Fisher Scientific
115 and ethanol (99.8%) was purchased from Fluka.

116 Monoclonal mouse anti-*Legionella* antibody Dp-Lp1-O2 provided by Microbiodetection
117 SARL (Commercy, France) was stored frozen, and three standard solutions were prepared
118 daily at 0.1, 0.05, and 0.01 mg/mL in HEPES-buffered saline (HBS) composed of 10 mM
119 HEPES and 150 mM NaCl.

120 All chemicals were analytical grade and were used without further purification.

121 **2.2. Bacterial strain**

122 A *Legionella pneumophila* sg1-GFP strain (Lp1-008-GFP) previously validated (Mustapha et
123 al., 2015) for the expression of green fluorescent protein (GFP) was cultured on buffered
124 charcoal yeast extract agar (BCYE α medium) containing chloramphenicol and incubated at
125 37 °C for 72 h to obtain exponential phase forms. All of the bacterial samples were freshly
126 prepared by resuspension of colonies in an appropriate volume of PBS (Dulbecco's
127 Phosphate-Buffered Solution, Sigma, France). An optical density (OD) of 0.2 at 600 nm
128 (Biomate TM3; Avantec, Illkirch, France) was taken as a reference for the initial suspension
129 containing 10^8 CFU/mL. Ten-fold serial dilutions from 10^8 to 10^0 CFU/ml were prepared and

130 used to study the biosensing performance in both static and dynamic detection mode. The
131 concentration of each independent initial suspension was determined by twice plating 100 μL
132 aliquots of 10^2 and 10^3 dilutions on BCYE agar medium. The *Legionella* colonies were
133 counted using a Scan 1200 enumerating system-Interscience, after 72 h at 37 °C.

134 **2.3. Apparatus**

135 All of the electrochemical measurements were performed at pH 7.4 in a 0.01 M PBS solution
136 containing 0.1 M KCl and 10 mM $[\text{Fe}(\text{CN})_6]^{3-/4-}$ (the reaction is controlled by diffusion of the
137 ferri/ferrocyanide system as a redox probe) using a portable bipotentiostat (Metrohm, France
138 SAS). Cyclic voltammograms (CV) were recorded at a scan range from -0.4 to +0.6 V with a
139 scan rate of 0.05 V/s. Square-wave voltammograms (SWV) were recorded from -0.3 to +0.5
140 V using the following parameters: a frequency of 5 Hz, a pulse amplitude of 0.002 V, and a
141 scan rate of 0.05 $\text{V}\cdot\text{s}^{-1}$. To guarantee reproducibility, each experiment was carried out
142 independently at least three times using three different SPEs. The Drop View 8400 software
143 plots the results as SWV and CV curves. The experiments were performed using a three-
144 electrode system with Au as the working electrode, Pt as the auxiliary electrode, and Ag as
145 the reference electrode.

146 Validation of functionalization was carried out by electrochemical measurements after each
147 functionalization step and by visualization of the morphological changes using scanning
148 electron microscopy (SEM, Nova Nanosem FEI 200, accelerating voltage 20 kV), and atomic
149 force microscopy (AFM, Agilent 5500 LS instrument, Les Ulis, France). Before being
150 observed by AFM, the SPEs were rinsed using ultrapure water and dried under nitrogen (N_2)
151 to prevent the formation of salt crystals. The images were processed using GWIDDION
152 software (version 2.52). The root mean square (RMS) was used to characterize the surface
153 roughness in terms of the irregularity and height distribution. Confocal laser scanning
154 microscopy (CLSM) images were obtained using a TCS-SP2 inverted confocal scanning laser
155 microscope (LEICA Microsystems, Nanterre, France), with argon as an excitation source (488
156 nm).

157 **2.4. Fabrication of the biosensor**

158 Screen-printed electrodes (SPEs), were purchased from Metrohm, France. The SPEs were
159 first rinsed with an acetone and ethanol solution to remove physically adsorbed contaminants.
160 The working area (4-mm diameter) was then immersed for 1 min in a fresh piranha solution
161 of 3:1 (v/v) 98% H_2SO_4 /30% H_2O_2 using all the necessary safety procedures. The SPEs were
162 then rinsed extensively with ultrapure water several times and finally dried in air.

163 Once cleaned, the SPEs were immersed in a solution of 2 mM 16-amino-1-hexadecanethiol
164 16-AHT in 99.8% ethanol for 24 hours in the dark at 4 °C to form self-assembled monolayers.
165 The carboxyl groups located on the crystallizable fragment of the heavy chains of the anti-
166 *L. pneumophila* monoclonal antibody (mAb) were activated using EDC (dissolved in MES) as
167 described by Vashist et al., 2011, 2015.

168 Despite its importance for the biosensing performance (Vashist, 2012; Vashist et al., 2011,
169 2015), it is still difficult to ensure the orientation of the antibody during the activation process.
170 According to the literature, the use of EDC (Ben Ismail et al., 2016; Vashist et al., 2015) or
171 EDC/N-hydroxysulfosuccinimide (NHS) (Chou et al., 2016; Raghav and Srivastava, 2016) or
172 EDC with Sulfo-NHS (Dixit et al., 2011) enables chemical activation of the carboxyl groups.
173 Thus, the antibody linkage occurs through a peptide bond that should, theoretically, not affect
174 its bioactivity.

175 However, the biosensor efficiency was found to be enhanced when EDC alone was used
176 (Vashist, 2012). We compared the use of EDC alone and the use of EDC along with NHS
177 (data not shown). The results corroborated the previous idea, which is a reason why we
178 adopted this method.

179 A 50 µL aliquot of the EDC-activated mAb antibodies was then incubated overnight at 4 °C.
180 A final step consisting of the addition of PBS containing 1% bovine serum albumin (BSA)
181 was carried out in order to block the non-specific binding sites on the sensing area.

182 ***2.5.Optimization of the antibody concentration under static conditions***

183 In order to be able to minimize the final cost of the biosensor, we tested the anti-*Legionella*
184 antibody at 3 different concentrations: 0.01, 0.05, and 0.1 mg/mL. These three concentrations
185 were tested to detect *Legionella* in static mode as follows: 10 µL of the dilution containing
186 *Legionella* at 10 CFUs/mL were deposited on the pretreated area of the SPE and then left for
187 3 h of incubation at room temperature and finally rinsed with PBS solution and characterized
188 electrochemically using CV and SWV. On the same biosensor, 10 µL of *Legionella* at 10²
189 CFUs/mL was added and the same procedure was performed, and so on, each time adding a
190 10-fold higher concentration of bacteria until *Legionella* at 10⁸ CFUs/mL was reached. This
191 procedure was used to obtain a more reliable indication of the occurrence of sensor saturation.

192 **As in our previous work regarding the detection of *Legionella* under static conditions (Souiri**
193 **et al., 2014), the sensor was incubated for 3 hours (Ben Ismail et al., 2016) so that the**
194 **bacterial cell capturing time could be considered to be long enough to assure a comparative**
195 **results with the dynamic mode of detection. The sensor was kept in a sealed empty Petri dish**
196 **to avoid surface dryness during the incubation.**

197

198

199 **2.6. Dynamic detection**

200 The *Legionella* detection experiments under dynamic conditions were carried out in a glove
201 box. The SPE was inserted into a microfluidic cell (volume of the cell: 8 μ L; Input Diameter:
202 1 mm - Metrohm, France) linked to a cell inlet and connected to the tube containing the
203 bacterial suspension (2 mL). Circulation was achieved using a peristaltic pump (Watson-
204 Marlow, type 101 U/R) and the bacterial suspensions were recirculated 5 times at a maximum
205 speed of 100 μ L.min⁻¹. The SPE electrode was then characterized electrochemically. The
206 dilutions were tested using the same cumulative process described for the static mode.

207 **2.7. Biosensing performance under dynamic conditions**

208 In order to evaluate the efficiency of this mode of detection, 2 mL aliquots of the pre-
209 circulated and the post-circulated contaminated samples were evaluated by culture: 500 μ L of
210 10, 10², and 10³ CFUs/mL samples were plated on four BCYE plates (eight plates for each
211 concentration). For each bacterial concentration, the initial suspension and the recirculated
212 suspension (total volume of 2 mL for each one) were plated on BCYE agar supplemented
213 with chloramphenicol and incubated at 37 °C for 72 h. All of the BCYE plates were observed
214 under UV light at 366 nm to enumerate GFP-*L. pneumophila* colonies. Flow cytometry assays
215 (FCA) (Cube6, Sysmex) were also carried out to assess the physiological states of the
216 bacteria: dead, alive, and 'viable but nonculturable' (VBNC) before and after fluid circulation.
217 The quantification protocol was as described in our previous study (Allegra et al., 2008).
218 Thus, 2 mL of 10⁵ CFU/mL was processed for quantification using this technique.

219 **3. Results and Discussion**

220 **3.1. Validation of the surface modification: layer formation**

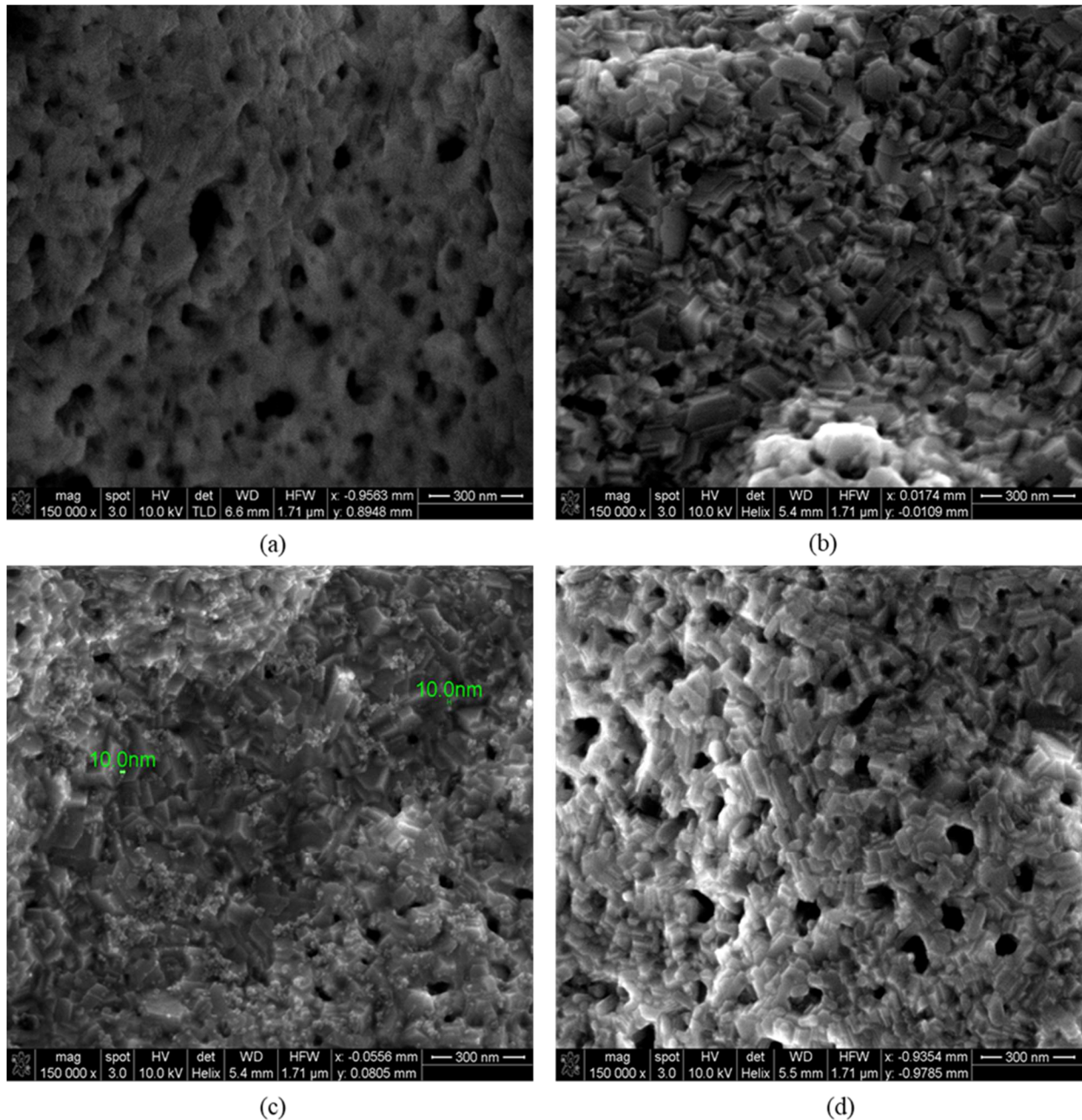
221 The subsequent functionalization steps carried out on the bare gold electrode successively
222 resulted in three modified surfaces: 16-AHT/Gold, mAb/16-AHT/Gold, and mAb-BSA/16-
223 AHT/Gold. Each of these three modified surfaces was characterized by microscopic imaging
224 techniques and by electrochemical measurements taking into account the responses obtained
225 with the bare gold surface.

226 **3.1.1. SEM and AFM characterization**

227 **a) SEM characterization**

228 SEM imaging was carried out on the bare gold surface (Fig. 1a) and on each of the three
229 subsequent modified surfaces (Fig. 1b, 1c, 1d). As can be seen in Fig. 1a, the surface
230 topography of the typical gold electrode exhibited a high level of definition and homogeneity

231 of the gold film. Compared to the SEM images of the bare gold surface, those obtained from
232 the functionalized surfaces revealed various new 'geometric shapes' that clearly indicated
233 effective immobilization of the corresponding molecules (16-AHT). In terms of the first
234 functionalization step (Fig. 1b), the corresponding geometric shapes appeared to be quite
235 smooth and the shapes had a narrow size range. Furthermore, this range did not change over
236 the entire surface. Such forms could be the result of organized self-assembled monolayers of
237 16-AHT (Fig. 1b). A similar result was previously reported by Heimel et al. (Heimel et al.,
238 2006) using the simulated adsorption geometry for 4'-substituted-4-mercaptobiphenyls. These
239 results suggest that the self-assembled molecules (SAM) can undergo a similar formation
240 process. The SEM image of the antibody-modified surface (0.1 mg/mL) revealed grainy
241 forms distributed homogeneously over the entire surface (Fig. 1c), suggesting successful mAb
242 linkage to the 16-AHT modified surface. As can be seen in Fig. 1d, the SEM image of the
243 BSA-treated surface (mAb-BSA/16-AHT/Gold) revealed the presence of more irregular
244 shapes that were between 20 and 50 nm in size. This could be attributed to the adsorption of
245 BSA on non-specific mAb binding areas. Our results, and those reported by others (Mathebe,
246 2004; Zhang et al., 2015), confirm the successful use of SEM imaging to characterize
247 modified surfaces during biosensor fabrication.



248
 249 *Figure 1. SEM images of bare Gold (a); 16-AHT/Gold (b); mAb/16-AHT/Gold (c), and mAb-BSA/16-*
 250 *AHT/Gold (d)*

251 ***b) AFM characterization***

252 The topography of the bare gold surface and each of the three modified surfaces was analysed
 253 using atomic force microscopy (AFM). The roughness parameter was evaluated as the
 254 average root mean square roughness (RMS) based on five measurements performed at five
 255 different locations ($2 \times 2 \mu\text{m}^2$) on the surface. The roughness of the bare gold surface differed
 256 from that obtained for the modified gold surface, suggesting the formation of layers of film on
 257 the gold surface. Depending on the functionalization step, the analysed surface exhibited a
 258 reduced RMS roughness with a substantial standard deviation. These results could be

259 explained by both the surface heterogeneity induced by the chemical modification and the
 260 manufacturing process of the screen-printing technology of gold particles suspended in an ink
 261 on a ceramic substrate (Butterworth et al., 2019). Yet, ultra-flat surfaces could be obtained
 262 using the pressure forming template stripping fabrication technique (0.35 ± 0.05 nm RMS
 263 roughness), as previously reported (Rubio-Lara et al., 2019). Overall, the generation of rough
 264 surfaces is one of the most convenient and effective ways to improve sensing signals (Gao et
 265 al., 2019). Following the first step of modification (16-AHT) of the gold substrate, the
 266 standard deviation decreased, suggesting good coverage of the modified surface. According to
 267 Love et al. (Love et al., 2005), SAMs can be fabricated into patterns in the plane of a surface
 268 with dimensions ranging from 10 to 100 nm, thus resulting in the formation of a geometric
 269 shape through the formation of an assembled monolayer. For the antibody modified surface,
 270 the slight decrease in the standard deviation could be the result of the immobilization of the
 271 antibody molecules. The addition of BSA appears to indicate better coverage of the surface,
 272 which could be due to the adsorption of BSA molecules at different angles, as previously
 273 reported (Rubio-Lara et al., 2019).

274

275 *Table 1. RMS value evaluation based on the AFM results ($2 \times 2 \mu\text{m}^2$)*

<i>Surface</i>	<i>RMS value \pmSD (nm)</i>
Bare gold	164 ± 75
16-AHT/Gold	149 ± 55
mAb/16-AHT /Gold	148 ± 73
mAb-BSA/16-AHT/Gold	131 ± 54

276

277 **3.1.2. Electrochemical characterization (SWV and CV)**

278 Electrochemical measurements remain the most effective method for surface analysis during
 279 the fabrication process and the performance of the biosensor. In our study, the electrochemical
 280 behaviour of the modified surface was investigated using square-wave voltammetry (SWV)
 281 and cyclic voltammetry (CV) of the bare gold electrode and the three subsequent
 282 modifications with 16-AHT, mAb, and BSA, respectively.

283 As can be seen in Fig.2, the peak current in SWV of the bare gold electrode was lower for
 284 each of the subsequent modified surfaces, suggesting immobilization of probe molecules. The

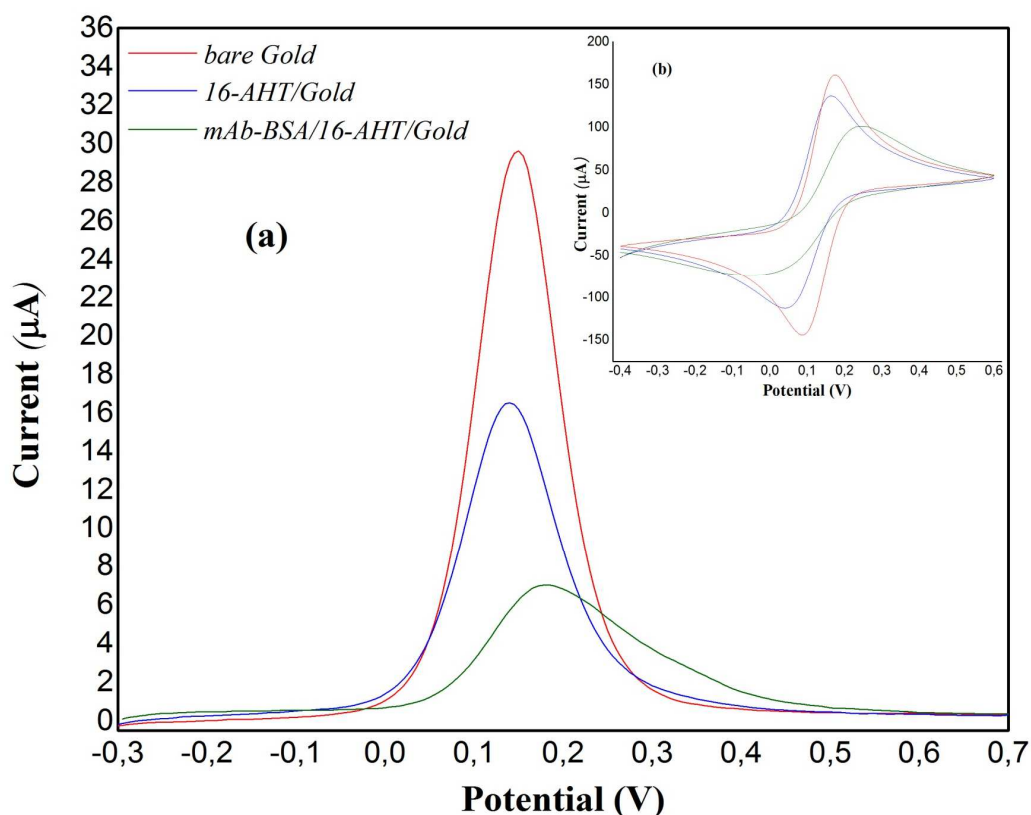
285 highest current response occurred for the gold electrode (red curve). The peak current
286 decreased substantially after treatment of the gold surface with aminothiols (blue
287 curve). The subsequent modification of the 16-AHT/Gold surface with antibody molecules
288 was associated with a further decrease in the corresponding peak current of SWV (green
289 curve), whereas no peak current change was observed after BSA treatment.

290 The observed decrease of the peak potentials by SWV after each of the two subsequent
291 functionalization steps of the bare gold electrode could be related to a restricted mass transfer
292 of redox species. This could be due to the molecular length of the covalently linked
293 aminothiols and mAb molecules (Chen et al., 2006; Zhang et al., 2014).

294 Furthermore, the reduction of the amplitudes of the current peaks recorded after the
295 functionalization steps was associated with a slight change in the peak potential location. The
296 peak current of the gold electrode was located at + 0.15 V whereas the peak current of the
297 aminothiols-treated electrode was shifted to + 0.13 V. This slight potential shift of the peak
298 current towards a lower voltage for the 16-AHT-modified surface could be related to the
299 presence of a positive electrostatic charge around the H₂N-terminated thiol-linked molecules.
300 Indeed, at the pH that was used (a pH of 7.4), and taking into account a pK_a of 10.6 for the
301 NH₃⁺/NH₂ couple (Kromann et al., 2016), the protonated form of the base predominated
302 (NH₃⁺). Moreover, the current peak for the treated surface with mAbs underwent a positive
303 shift relative to that obtained following the first functionalization step. The corresponding
304 peak appeared at + 0.18 V. This additional shift could be the result of the negative charge of
305 the mAbs carboxyl groups at pH = 7.4. The negative charges introduced after mAb treatment
306 would neutralize the positive charges of the amino functional groups. This could explain the
307 shift of the current peak to a higher voltage following the second step of the functionalization
308 of the biosensor. Similar results have been reported based on electrochemical impedance
309 spectroscopy (Sboui et al., 2015). **The changes noted with SWV were confirmed by cyclic
310 voltammetry. The same variation was found in the characterized signals as discussed for the
311 SWV results. Of note, there was a greater decrease of the peak current with SWV compared
312 to CV. This could be due to the sensitivity of the SWV technique. Indeed, SWV measures
313 both the forward and the reverse current, while only the forward current is measured in CV
314 (Brahman et al., 2016).**

315 All of these microscopic and electrochemical measurements suggest that the functionalization
316 steps during the biosensor fabrication were successful. These data are in agreement with the
317 results of the immunofluorescence experiment, which was carried out to make sure that the

318 bioreceptor recognition sites were still accessible after the addition of BSA (using an Alexa
319 Fluor 555 antibody, data not shown).
320



321
322 *Figure 2. Square-wave voltammetry (a) and cyclic voltammetry (b) of the modified electrode*
323 *of bare Gold (red), 16-AHT/Gold (blue), and mAb-BSA/16-AHT/Gold (green)*

324

325 **3.2. Antibody concentration optimization under static conditions**

326 The aim of this part of the study was to estimate the lowest antibody concentration that would
327 still ensure a linear electrochemical response, under static conditions, for bacterial
328 suspensions ranging from 10 to 10⁸ CFU/mL (as described in Section 2.4). Thus, three
329 antibody concentrations of 0.01 mg/mL, 0.05 mg/mL, and 0.1 mg/mL were successively
330 investigated.

331 The biosensor current signals needed for this study were, $I_{\text{mAb-BSA}}$ and $I_{\text{detection}}$, which were
332 the recorded signals without bacteria and the bacterial concentrations, respectively. These
333 recorded signals permitted us to calculate the $\Delta I/I$ as $[I_{\text{(mAb-BSA)}} - I_{\text{(detection)}}] / I_{\text{(mAb-BSA)}}$. For
334 each of the three antibody concentrations, a plot of the $\Delta I/I$ values versus the logarithm of the
335 *Legionella* concentration is represented in Figure 3.

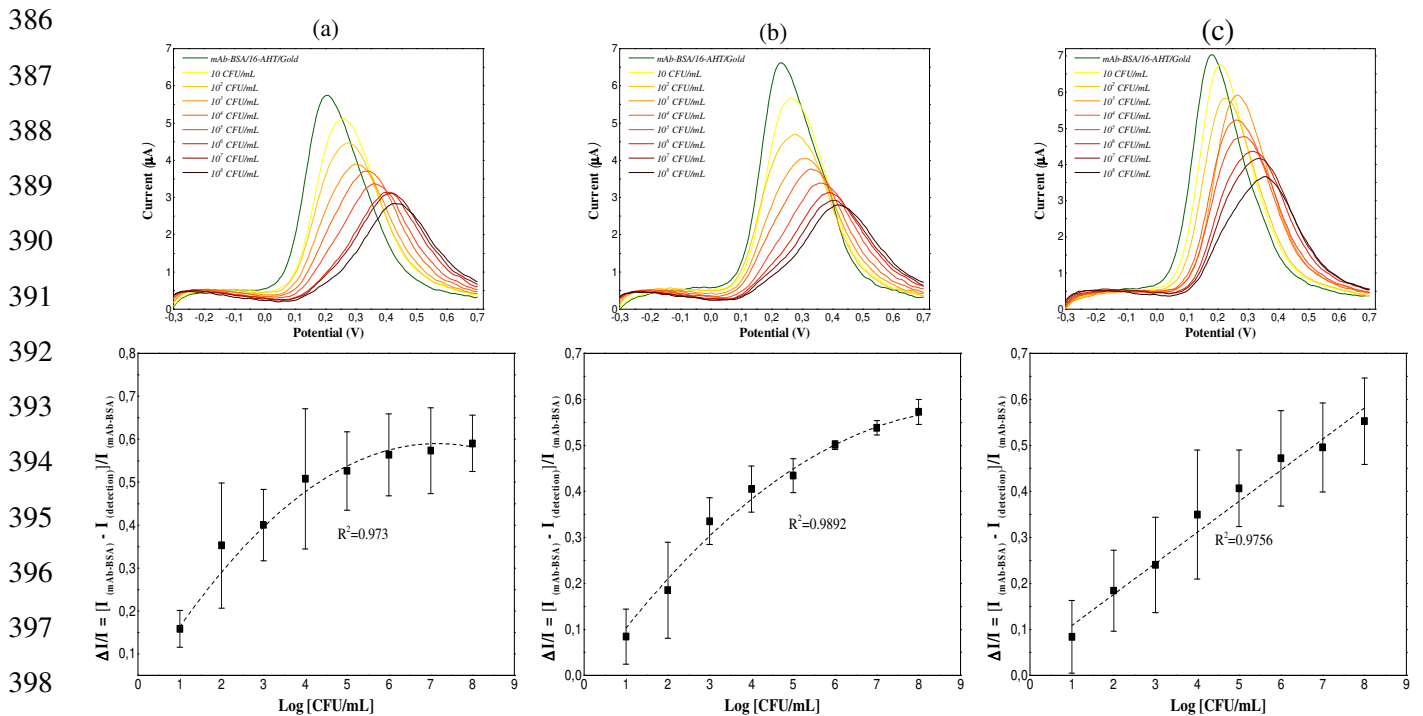
336 As expected, there was a decrease in $I_{\text{detection}}$ due to bacterial capture, and thus an increase in
337 the $\Delta I/I$ values as the bacterial concentration increased. The observed increase in the $\Delta I/I$
338 values could be attributed to the immobilization of bacterial cells, which acted as a barrier to
339 electron transfer reactions on the biosensing surface. Such an impediment of the electron
340 transfer kinetics on the electrode surface has been shown to occur during the formation of
341 antibody/antigen complexes (Yun et al., 2007; Zhang et al., 2014). In order to confirm the
342 immobilization of captured GFP-*L. pneumophila*, CLSM was performed. As shown in Fig.3d,
343 the images obtained indicate a homogeneous distribution of the captured bacterial cells at an
344 antibody concentration of 0.1 mg/mL.

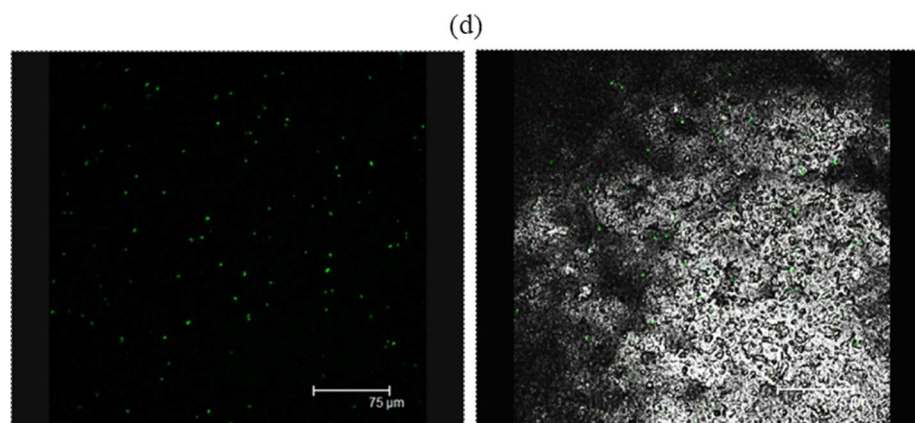
345 As can be seen in Fig. 3a and Fig. 3b, the $\Delta I/I$ values corresponding to antibody
346 concentrations of 0.01 and 0.05 mg/mL did not increase in a linear manner with a *Legionella*
347 concentration range from 10 to 10^8 CFU/mL. A saturation phenomenon was observed at these
348 two antibody concentrations as the number of *Legionella* increased. By contrast, at an
349 antibody concentration of 0.1 mg/mL (Fig. 3c), a linear increase in $\Delta I/I$ values was observed
350 over a bacterial concentration range from 10 to 10^8 CFU/mL ($R^2 = 0.975$).

351 Therefore, under static conditions, the electrochemical biosensor functionalized with an
352 antibody concentration of 0.1 mg/mL exhibited a wide linear response that ranged from 10 to
353 10^8 CFU/mL.

354 At an antibody concentration of 0.1 mg/mL, the limit of detection (LOD) was calculated to be
355 $3 \times \text{SD}$ (SD: standard deviation, $n = 3$) obtained from three measurements taken in the absence
356 of bacteria. Three peak currents were recorded in the absence of *Legionella*, with values of
357 7.22 (I_1), 7.02 (I_2), and 5.9 μA (I_3), with a mean value of 6.72 μA (I_0). Each of these three
358 values (I_1 , I_2 , and I_3) was then used to obtain the corresponding immunosensor response in the
359 absence of bacteria evaluated as $|I_0 - I|/I_0$. The values for the three responses obtained were:
360 0.075, 0.044, and 0.122, with a mean value of 0.08 and an SD value of 0.04. Therefore, the
361 LOD was calculated to be $3 \times \text{SD}$, thus yielding a value of 0.12 with regard to the
362 immunoresponse. The corresponding LOD value expressed in CFU/mL was then obtained
363 from the calibration curve (Fig. 3c), yielding a value of ~ 10 CFU/mL. This LOD value was
364 expected since the immunosensor responses varied linearly with the logarithmic value of the
365 bacterial concentration over eight orders of magnitude (Fig. 3c), which included 10 CFU/mL.
366 This LOD value is at least one order of magnitude lower than the values reported to date for
367 the detection of *Legionella pneumophila* using various other biosensing devices. Compared to
368 the previously published works discussed in the Introduction, our immunosensor appears to be
369 the best device to detect *Legionella pneumophila* at 10 CFU/mL. Moreover, our method has

370 the advantage of a relatively rapid analysis time (180 min), in addition to being portable, easy
 371 to operate, and relatively inexpensive compared to the other available technologies. Despite
 372 the excellent LOD value that we obtained and these advantages, this detection limit remains
 373 quite high compared to the reference levels for cooling towers (< 100 CFU/L) (Miranda-
 374 Castro et al., 2009) and thus needs to be improved. Another hurdle to be overcome is that this
 375 LOD is subject to the weakness of the corresponding response. As described above, the blank
 376 assay was associated with a biosensing response of $[\Delta I/I]_{\text{Blank}} = 0.08 \pm 0.04$. Otherwise, the
 377 immunosensor response with *Legionella* at 10 CFU/mL ($[\Delta I/I]_{10 \text{ CFU/mL}}$), obtained as the mean
 378 of three simultaneously measurements, was 0.08 ± 0.08 . Thus, both of the $[\Delta I/I]_{\text{Blank}}$ and
 379 $[\Delta I/I]_{10 \text{ CFU/mL}}$ responses were nearly the same.
 380 This result suggests that 10 CFU/mL corresponds to the limit of detection of *Legionella* under
 381 static conditions, and this is in agreement with the obtained LOD ($3 \times \text{SD}$). Nevertheless, due
 382 to the weakness of the response value and the relatively high SD, it would not be easy to
 383 detect 10 CFU/mL every time. Thus, increasing the response value of 10 CFU/mL by
 384 changing the detection conditions could be of great interest. Such an improvement would
 385 result in a more efficient quantification of 10 CFU/mL.





399

400 *Figure 3. SWV net currents and sensor performance for antibody concentrations of 0.01*
 401 *mg/mL (a), 0.05 mg/mL (b), and 0.1 mg/mL (c) under static conditions. A CLSM image of*
 402 *captured GFP-L. pneumophila (left) and a CLSM image of captured GFP-L. pneumophila*
 403 *with reflectance mode (right) using an antibody concentration of 0.1 mg/mL (d)*

404

405 **3.3. Performance of the dynamic biosensor**

406 **a- Electrochemical characterization**

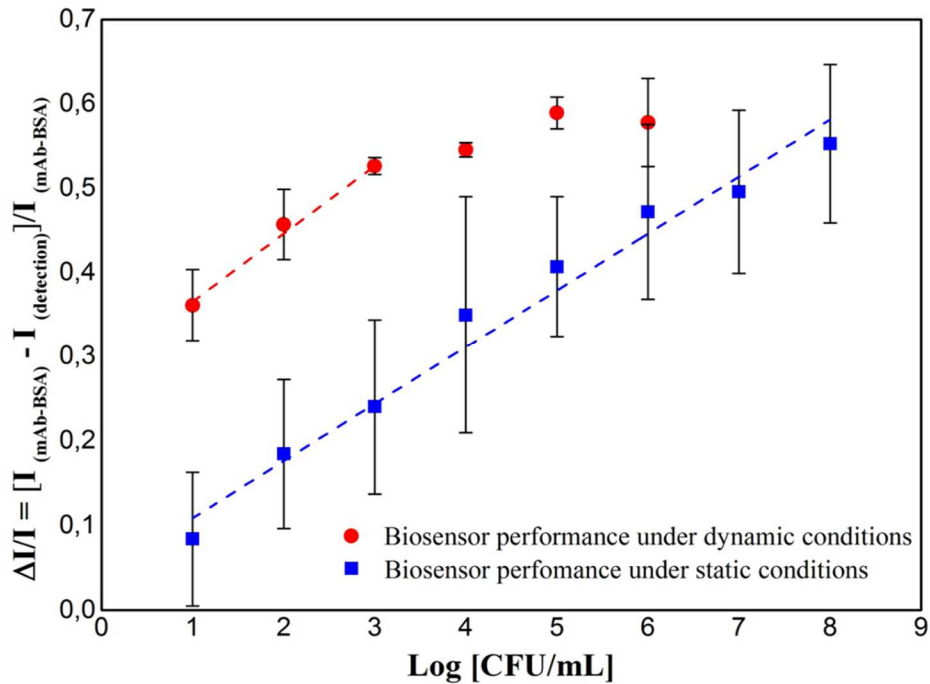
407 The biosensor described above was used to perform electrochemical measurements to detect
 408 and quantify *Legionella* present in circulating solutions (dynamic conditions). The aim was to
 409 achieve a **faster response time and amplified signal sensing** compared to measurements
 410 performed under static conditions as discussed previously.

411 **The biosensor was coupled to the microfluidic system as described in Section 2.6. The**
 412 **biosensor measurements were performed under dynamic conditions with an antibody**
 413 **concentration of 0.1 mg/mL. A plot of $\Delta I/I$ values vs. the logarithm of a *Legionella***
 414 **concentration ranging from 10 to 10⁶ CFU/mL is shown in Fig. 4 (red curve). It can be seen**
 415 **that, compared to the sensor performance under static conditions (blue curve), the**
 416 **performance under dynamic conditions (red curve) indicates an amplified biosensing**
 417 **response. Furthermore, a linear increase in the $\Delta I/I$ values was only observed up to 10³**
 418 **CFU/mL. Between 10³ CFU/mL and 10⁶ CFU/mL the representative curve trended downward**
 419 **and tended to plateau, whereas the $\Delta I/I$ values measured under static conditions revealed a**
 420 **linear increase over the entire 10 to 10⁸ CFU/mL bacterial concentration range. This finding**
 421 **illustrates the precocious appearance of a saturation phenomenon when the biosensor was**
 422 **used under dynamic conditions. Moreover, as can be seen in Fig. 4, the linear part of the curve**
 423 **established under dynamic conditions ($R^2=0.991$) was almost parallel to the linear**
 424 **representation obtained under static conditions. Considering that biosensor sensitivity is**

425 defined as the slope of the linear part of the calibration curve, our results suggest that the
426 sensitivity of the biosensor under dynamic conditions remains almost the same as the
427 sensitivity observed under static conditions. Circulation of each of the three bacterial
428 concentrations (10 , 10^2 , and 10^3 CFU/mL) led to a nearly 4.5-fold increase in the $\Delta I/I$ values
429 relative to the $\Delta I/I$ values obtained under static conditions., namely $[\Delta I/I]_{10 \text{ CFU/mL}} = 0.361 \pm$
430 0.04 . The enhancement of the immunosensing response by the use of this microfluidic system
431 suggests that it should be possible to use this biosensor under dynamic conditions to quantify
432 *Legionella* at very low concentrations ranging from 10 to 10^3 CFU/mL. Due to the 4.5-fold
433 increase in the immunosensing response achieved with circulation, a bacterial concentration
434 of 10 CFU/mL can more readily be detected under dynamic conditions. In light of this, our
435 method based on the use of circulating bacteria appears to be more suitable for quantification
436 of *Legionella pneumophila* at a concentration of 10 CFU/mL. In addition, it seems likely that
437 the detection limit should be significantly lower compared to the LOD obtained under static
438 conditions. Furthermore, the incubation time with the bacteria was reduced from 180 min
439 under static conditions to 100 min under dynamic conditions. The enhancement in the
440 immunosensing response under dynamic conditions may be attributed to the increase in the
441 number of cells captured by recirculation of the *Legionella* samples. This is, on the one hand,
442 directly linked to a higher probability of contact between the bacteria cells and the
443 functionalized surface and, on the other hand, it explains the occurrence of a precocious
444 saturation phenomenon under dynamic conditions.

445 Moreover, linearity was not sought for bacterial samples at high concentrations since the aim
446 of this study was to detect and quantify *Legionella* at very low concentrations. In France, the
447 law of the decree of February 1st, 2010 (Arrêté du 1^{er} février 2010, n.d.) specifies that target
448 values of 10^3 CFU/L in public entities and 10 CFU/L in healthcare institutions should be used
449 for *Legionella* risk assessment.

450



451

452 *Figure 4. Sensor performance: performance comparison between dynamic conditions (red*
 453 *curve) and static conditions (blue curve)*

454

455

456 ***b- Physiological state of Legionella under dynamic conditions***

457 In order to evaluate the impact of dynamic conditions on the physiological state of *Legionella*,
 458 culture and flow cytometry measurements were performed.

459 FCA (as described in Section 2.7), was applied to a bacterial concentration of 10⁵ CFU/mL.

460 The percentage of dead cells before and after sample circulation was almost the same: 27%
 461 for the bacterial cell input (the precirculated aqueous sample) and 29% after dynamic
 462 detection. Thus, these results indicate that the microfluidic system did not affect the viability
 463 of the *Legionella* cells under dynamic conditions. Moreover, similar to the results obtained by
 464 the culture method, the FCA results confirm, as in our previous study (Sboui et al., 2015), that
 465 viable and culturable cells as well as viable but nonculturable cells were captured by the
 466 biosensor with the same degree of efficacy.

467 Table 2 presents the number of colonies for the three *Legionella* concentrations ranging from
 468 10 to 10³ CFU/mL. When performed with the precirculated aqueous samples, 15, 96, and 945
 469 colonies were enumerated for the corresponding theoretical concentration of 10, 10², and 10³
 470 CFU/mL, respectively. For these three bacterial concentrations, the plates incubated with
 471 recirculated solutions had 5, 45, and 601 enumerated colonies, respectively. Thus, these

472 results indicate a decrease in the number of enumerated colonies when the cultures were
 473 performed with recirculated solutions compared to cultures performed prior to circulation.
 474 Percentage-wise, these decreases were 67%, 53%, and 36%, respectively. The decrease in
 475 *Legionella* cells in the circulated solutions could result in more bacterial cells being captured,
 476 thereby leading to enhancement of the biosensing signals with regard to $\Delta I/I$ values.
 477 As described above, a similar linear relationship was found between the $\Delta I/I$ values and the
 478 logarithm of the bacterial concentration ranging from 10 to 10^3 CFU/mL. Moreover, we found
 479 a linear relationship by plotting the percentage of captured cells and the logarithm of the
 480 corresponding concentrations ($R^2 = 0.996$). These two linear relationships suggest that the $\Delta I/I$
 481 values were correlated to the percentage decrease in the number of colonies ($R^2 = 0.977$).
 482 Therefore, it can be assumed that the increase in $\Delta I/I$ values was due to the greater extent of
 483 *Legionella* capture under dynamic conditions.

489 *Table 2. Post-quantitative assessment of Legionella in recirculated artificially contaminated samples*
 490 *by culture*

<i>Theoretical concentrations based on OD measurements</i>	<i>Enumerated colonies by culture: based on the number of the non-stressed (live) bacteria</i>		
	<u>Before circulation</u> (CFU/mL)	<u>After circulation</u> (CFU/mL)	<u>Percentage decrease</u>
10	15	5	67%
10^2	96	45	53%
10^3	945	601	36%

4. Conclusion

505 An electrochemical method was developed by coupling a functionalized biosensor with a
506 microfluidic cell for the detection of *Legionella pneumophila* sg1 in water samples. The main
507 functionalization steps of the biosensor were performed by covalent linkage of a self-
508 assembled monolayer of 16-amino-1-hexadecanethiol (16-AHT) onto a gold surface to
509 immobilize an anti-*L. pneumophila* monoclonal antibody (mAb). Characterization by
510 electrochemical methods and microscopic imaging techniques indicated immobilization of
511 both the mAb and the targeted bacteria. Under static conditions, the biosensor exhibited a
512 wide linear response range from 10 to 10⁸ CFU/mL and a detection limit of 10 CFU/mL.
513 Using a microfluidic system, a linear biosensing signal was obtained between 10 and 10³
514 CFU/mL, with a response amplification by a factor of 4.5 compared to the results under static
515 conditions. Thus, the observed enhancement of the biosensor response should result in a better
516 detection limit: less than 10 CFU/mL. Therefore, the use of this combination for
517 electrochemical detection of *Legionella* cells has several advantages such as sensitivity, good
518 response amplification, an easy fabrication process, a faster method, real-time detection, and
519 portability. There is hence ample potential to expand the application of this biosensor
520 configuration to assess the risk of *Legionella* bacterial contamination in environmental water
521 systems, and a real-time biosensing signal could be of practical value in this field, especially
522 during epidemics.

523

524 ***Acknowledgments***

525 The authors gratefully acknowledge financial support from the Region Rhône Alpes - CMIRA
526 program. A special thanks to the late Prof. Serge RIFFARD who played a key role in
527 spearheading this work.

528 The authors also thank the laboratory team of the GIMAP and Hubert Curien (Saint-Étienne,
529 France) for their technical assistance.

530

531 ***References***

532 Allegra, S., Berger, F., Berthelot, P., Grattard, F., Pozzetto, B., Riffard, S., 2008. Use of Flow
533 Cytometry To Monitor *Legionella* Viability. *Appl. Environ. Microbiol.* 74, 7813–
534 7816. <https://doi.org/10.1128/AEM.01364-08>

535 Allegra, S., Grattard, F., Girardot, F., Riffard, S., Pozzetto, B., Berthelot, P., 2011.
536 Longitudinal Evaluation of the Efficacy of Heat Treatment Procedures against
537 *Legionella* spp. in Hospital Water Systems by Using a Flow Cytometric Assay. *Appl.*
538 *Environ. Microbiol.* 77, 1268–1275. <https://doi.org/10.1128/AEM.02225-10>

539 Alleron, L., Khemiri, A., Koubar, M., Lacombe, C., Coquet, L., Cosette, P., Jouenne, T.,
540 Frere, J., 2013. VBNC *Legionella pneumophila* cells are still able to produce virulence
541 proteins. *Water Res.* 47, 6606–6617. <https://doi.org/10.1016/j.watres.2013.08.032>
542 Arrêté du 1er février 2010, n.d. Arrêté du 1er février 2010 relatif à la surveillance des
543 légionelles dans les installations de production, de stockage et de distribution d'eau
544 chaude sanitaire. NOR: SASP1002960A. URL :
545 [https://www.legifrance.gouv.fr/affichTexte.do?cidTexte=JORFTEXT000021795143&](https://www.legifrance.gouv.fr/affichTexte.do?cidTexte=JORFTEXT000021795143&categorieLien=id)
546 [categorieLien=id](https://www.legifrance.gouv.fr/affichTexte.do?cidTexte=JORFTEXT000021795143&categorieLien=id). Last accessed on July 2019.

547 Aziziyani, M.R., Hassen, W.M., Sharma, H., Shirzaei Sani, E., Annabi, N., Frost, E.H.,
548 Dubowski, J.J., 2020. Sodium dodecyl sulfate decorated *Legionella pneumophila* for
549 enhanced detection with a GaAs/AlGaAs nanoheterostructure biosensor. *Sens.*
550 *Actuators B Chem.* 304, 127007. <https://doi.org/10.1016/j.snb.2019.127007>

551 Baldovin, T., Pierobon, A., Bertonecello, C., 2018. May car washing represent a risk for
552 *Legionella* infection? *Ann. Ig. Med. Prev. E Comunità* 57–65.
553 <https://doi.org/10.7416/ai.2018.2196>

554 Beer, K.D., Gargano, J.W., Roberts, V.A., Hill, V.R., Garrison, L.E., Kutty, P.K., Hilborn,
555 E.D., Wade, T.J., Fullerton, K.E., Yoder, J.S., 2015. Surveillance for Waterborne
556 Disease Outbreaks Associated with Drinking Water - United States, 2011-2012.
557 *MMWR Morb. Mortal. Wkly. Rep.* 64, 842–848.

558 Ben Ismail, M., Carreiras, F., Agniel, R., Mili, D., Sboui, D., Zanina, N., Othmane, A., 2016.
559 Application of APTES-Anti-E-cadherin film for early cancer monitoring. *Colloids*
560 *Surf. B Biointerfaces* 146, 550–557. <https://doi.org/10.1016/j.colsurfb.2016.06.048>

561 Borella, P., Guerrieri, E., Marchesi, I., Bondi, M., Messi, P., 2005. Water ecology of
562 *Legionella* and protozoan: environmental and public health perspectives, in:
563 *Biotechnology Annual Review*. Elsevier, pp. 355–380. [https://doi.org/10.1016/S1387-](https://doi.org/10.1016/S1387-2656(05)11011-4)
564 [2656\(05\)11011-4](https://doi.org/10.1016/S1387-2656(05)11011-4)

565 Brahman, P.K., Pandey, N., Kumar, J.V.S., Somarouthu, P., Tiwari, S., Pitre, K.S., 2016.
566 Highly sensitive stripping voltammetric determination of a biomolecule, pyruvic acid
567 in solubilized system and biological fluids. *Arab. J. Chem.* 9, S1897–S1904.
568 <https://doi.org/10.1016/j.arabjc.2014.02.003>

569 Butterworth, A., Blues, E., Williamson, P., Cardona, M., Gray, L., Corrigan, D.K., 2019.
570 SAM Composition and Electrode Roughness Affect Performance of a DNA Biosensor
571 for Antibiotic Resistance. *Biosensors* 9, 22. <https://doi.org/10.3390/bios9010022>

572 Campese, C., 2018. Christine, C., 2018. Légionellose 2018 : point de situation au 9 juillet
573 2018. Christine Campese (christine.campese@santepubliquefrance.fr, Direction des
574 maladies infectieuses. Unité des infections respiratoires et vaccination, Agence
575 nationale de santé publique France 12 rue du Val d'Osne 94415 Saint-Maurice Cedex
576 France – Standard +33 (0)1 41 79 67 00), [https://www.srlf.org/wp-](https://www.srlf.org/wp-content/uploads/2018/07/Legionellose-bilan-2018-au-09-07-2018.pdf)
577 [content/uploads/2018/07/Legionellose-bilan-2018-au-09-07-2018.pdf](https://www.srlf.org/wp-content/uploads/2018/07/Legionellose-bilan-2018-au-09-07-2018.pdf). Last accessed
578 on July 2019.

579 Chang, C.-W., Hwang, Y.-H., Cheng, W.-Y., Chang, C.-P., 2007. Effects of chlorination and
580 heat disinfection on long-term starved *Legionella pneumophila* in warm water. *J.*
581 *Appl. Microbiol.* 102, 1636–1644. <https://doi.org/10.1111/j.1365-2672.2006.03195.x>

582 Chen, F., Li, X., Hihath, J., Huang, Z., Tao, N., 2006. Effect of Anchoring Groups on Single-
583 Molecule Conductance: Comparative Study of Thiol-, Amine-, and Carboxylic-Acid-
584 Terminated Molecules. *J. Am. Chem. Soc.* 128, 15874–15881.
585 <https://doi.org/10.1021/ja065864k>

586 Chou, Y.-N., Sun, F., Hung, H.-C., Jain, P., Sinclair, A., Zhang, P., Bai, T., Chang, Y., Wen,
587 T.-C., Yu, Q., Jiang, S., 2016. Ultra-low fouling and high antibody loading
588 zwitterionic hydrogel coatings for sensing and detection in complex media. *Acta*
589 *Biomater.* 40, 31–37. <https://doi.org/10.1016/j.actbio.2016.04.023>

590 Delgado-Viscogliosi, P., Simonart, T., Parent, V., Marchand, G., Dobbelaere, M., Pierlot, E.,
591 Pierzo, V., Menard-Szczebara, F., Gaudard-Ferveur, E., Delabre, K., Delattre, J.M.,
592 2005. Rapid Method for Enumeration of Viable *Legionella pneumophila* and Other
593 *Legionella* spp. in Water. *Appl. Environ. Microbiol.* 71, 4086–4096.
594 <https://doi.org/10.1128/AEM.71.7.4086-4096.2005>

595 Dietersdorfer, E., Kirschner, A., Schrammel, B., Ohradanova-Repic, A., Stockinger, H.,
596 Sommer, R., Walochnik, J., Cervero-Aragó, S., 2018. Starved viable but non-
597 culturable (VBNC) *Legionella* strains can infect and replicate in amoebae and human
598 macrophages. *Water Res.* 141, 428–438. <https://doi.org/10.1016/j.watres.2018.01.058>

599 Dixit, C.K., Vashist, S.K., MacCraith, B.D., O’Kennedy, R., 2011. Multisubstrate-compatible
600 ELISA procedures for rapid and high-sensitivity immunoassays. *Nat. Protoc.* 6, 439–
601 445. <https://doi.org/10.1038/nprot.2011.304>

602 Dooling, K.L., Toews, K.-A., Hicks, L.A., Garrison, L.E., Bachaus, B., Zansky, S., Carpenter,
603 L.R., Schaffner, B., Parker, E., Petit, S., Thomas, A., Thomas, S., Mansmann, R.,
604 Morin, C., White, B., Langley, G.E., 2015. Active Bacterial Core Surveillance for
605 Legionellosis — United States, 2011–2013. *MMWR Morb. Mortal. Wkly. Rep.* 64,
606 1190–1193. <https://doi.org/10.15585/mmwr.mm6442a2>

607 Enrico, D.L., Manera, M.G., Montagna, G., Cimaglia, F., Chiesa, M., Poltronieri, P., Santino,
608 A., Rella, R., 2013. SPR based immunosensor for detection of *Legionella*
609 *pneumophila* in water samples. *Opt. Commun.* 294, 420–426.
610 <https://doi.org/10.1016/j.optcom.2012.12.064>

611 Foudeh, A.M., Brassard, D., Tabrizian, M., Veres, T., 2015. Rapid and multiplex detection of
612 *Legionella*’s RNA using digital microfluidics. *Lab. Chip* 15, 1609–1618.
613 <https://doi.org/10.1039/C4LC01468E>

614 Gao, Y., Sun, S., Shi, S.-Q., Ciucci, F., Zhang, T.-Y., 2019. On-chip suspended gold nanowire
615 electrode with a rough surface: Fabrication and electrochemical properties.
616 *Electrochimica Acta* 304, 20–29. <https://doi.org/10.1016/j.electacta.2019.02.106>

617 Heimel, G., Romaner, L., Brédas, J.-L., Zojer, E., 2006. Interface Energetics and Level
618 Alignment at Covalent Metal-Molecule Junctions: π -Conjugated Thiols on Gold.
619 *Phys. Rev. Lett.* 96. <https://doi.org/10.1103/PhysRevLett.96.196806>

620 Kirschner, A.K.T., 2016. Determination of viable legionellae in engineered water systems: Do
621 we find what we are looking for? *Water Res.* 93, 276–288.
622 <https://doi.org/10.1016/j.watres.2016.02.016>

623 Kromann, J.C., Larsen, F., Moustafa, H., Jensen, J.H., 2016. Prediction of pKa values using
624 the PM6 semiempirical method. *PeerJ* 4, e2335. <https://doi.org/10.7717/peerj.2335>

625 Lei, K.F., Leung, P.H.M., 2012. Microelectrode array biosensor for the detection of
626 *Legionella pneumophila*. *Microelectron. Eng.* 91, 174–177.
627 <https://doi.org/10.1016/j.mee.2011.10.002>

628 Li, N., Brahmendra, A., Veloso, A.J., Prashar, A., Cheng, X.R., Hung, V.W.S., Guyard, C.,
629 Terebiznik, M., Kerman, K., 2012. Disposable Immunochips for the Detection of
630 *Legionella pneumophila* Using Electrochemical Impedance Spectroscopy. *Anal.*
631 *Chem.* 84, 3485–3488. <https://doi.org/10.1021/ac3003227>

632 Lin, H.-Y., Tsao, Y.-C., Tsai, W.-H., Yang, Y.-W., Yan, T.-R., Sheu, B.-C., 2007.
633 Development and application of side-polished fiber immunosensor based on surface
634 plasmon resonance for the detection of *Legionella pneumophila* with halogens light
635 and 850nm-LED. *Sens. Actuators Phys.* 138, 299–305.
636 <https://doi.org/10.1016/j.sna.2007.05.015>

637 Love, J.C., Estroff, L.A., Kriebel, J.K., Nuzzo, R.G., Whitesides, G.M., 2005. Self-Assembled
638 Monolayers of Thiolates on Metals as a Form of Nanotechnology. *Chem. Rev.* 105,
639 1103–1170. <https://doi.org/10.1021/cr0300789>

640 Martín, M., Salazar, P., Jiménez, C., Lecuona, M., Ramos, M.J., Ode, J., Alcoba, J., Roche,
641 R., Villalonga, R., Campuzano, S., Pingarrón, J.M., González-Mora, J.L., 2015. Rapid
642 *Legionella pneumophila* determination based on a disposable core–shell Fe₃O₄
643 @poly(dopamine) magnetic nanoparticles immunoplatfom. *Anal. Chim. Acta* 887,
644 51–58. <https://doi.org/10.1016/j.aca.2015.05.048>

645 Mathebe, N., 2004. Electrochemistry and scanning electron microscopy of
646 polyaniline/peroxidase-based biosensor. *Talanta* 64, 115–120.
647 <https://doi.org/10.1016/j.talanta.2003.11.050>

648 Miranda-Castro, R., de-los-Santos-Álvarez, N., Lobo-Castañón, M.J., Miranda-Ordieres, A.J.,
649 Tuñón-Blanco, P., 2009. PCR-coupled electrochemical sensing of *Legionella*
650 *pneumophila*. *Biosens. Bioelectron.* 24, 2390–2396.
651 <https://doi.org/10.1016/j.bios.2008.12.014>

652 Mobed, A., Baradaran, B., Guardia, M. de la, Agazadeh, M., Hasanzadeh, M., Rezaee, M.A.,
653 Mosafer, J., Mokhtarzadeh, A., Hamblin, M.R., 2019a. Advances in detection of
654 fastidious bacteria: From microscopic observation to molecular biosensors. *TrAC*
655 *Trends Anal. Chem.* 113, 157–171. <https://doi.org/10.1016/j.trac.2019.02.012>

656 Mobed, A., Hasanzadeh, M., Babaie, P., Agazadeh, M., Mokhtarzadeh, A., Rezaee, M.A.,
657 2019b. DNA-based bioassay of legionella pneumonia pathogen using gold
658 nanostructure: A new platform for diagnosis of legionellosis. *Int. J. Biol. Macromol.*
659 128, 692–699. <https://doi.org/10.1016/j.ijbiomac.2019.01.125>

660 Mustapha, P., Epalle, T., Allegra, S., Girardot, F., Garraud, O., Riffard, S., 2015. Monitoring
661 of *Legionella pneumophila* viability after chlorine dioxide treatment using flow
662 cytometry. *Res. Microbiol.* 166, 215–219.
663 <https://doi.org/10.1016/j.resmic.2015.01.004>

664 Orkis, L.T., Harrison, L.H., Mertz, K.J., Brooks, M.M., Bibby, K.J., Stout, J.E., 2018.
665 Environmental sources of community-acquired legionnaires' disease: A review. *Int. J.*
666 *Hyg. Environ. Health* 221, 764–774. <https://doi.org/10.1016/j.ijheh.2018.04.013>

667 Raghav, R., Srivastava, S., 2016. Immobilization strategy for enhancing sensitivity of
668 immunosensors: L -Asparagine–AuNPs as a promising alternative of EDC–NHS

669 activated citrate–AuNPs for antibody immobilization. *Biosens. Bioelectron.* 78, 396–
670 403. <https://doi.org/10.1016/j.bios.2015.11.066>

671 Rai, V., Nyine, Y.T., Hapuarachchi, H.C., Yap, H.M., Ng, L.C., Toh, C.-S., 2012.
672 Electrochemically amplified molecular beacon biosensor for ultrasensitive DNA
673 sequence-specific detection of *Legionella* sp. *Biosens. Bioelectron.* 32, 133–140.
674 <https://doi.org/10.1016/j.bios.2011.11.046>

675 Rubio-Lara, J.A., Bergler, F., Attwood, S.J., Edwardson, J.M., Welland, M.E., 2019. Ultraflat
676 Gold QCM Electrodes Fabricated with Pressure-Forming Template Stripping for
677 Protein Studies at the Nanoscale. *Langmuir.*
678 <https://doi.org/10.1021/acs.langmuir.8b03782>

679 Sboui, D., Souiri, M., Reynaud, S., Palle, S., Ismail, M.B., Epalle, T., Mzoughi, R., Girardot,
680 F., Allegra, S., Riffard, S., Othmane, A., 2015. Characterisation of electrochemical
681 immunosensor for detection of viable not-culturable forms of *Legionella pneumophila*
682 in water samples. *Chem. Pap.* 69. <https://doi.org/10.1515/chempap-2015-0170>

683 Sharma, L., Losier, A., Tolbert, T., Dela Cruz, C.S., Marion, C.R., 2017. Atypical Pneumonia.
684 *Clin. Chest Med.* 38, 45–58. <https://doi.org/10.1016/j.ccm.2016.11.011>

685 Soda, E.A., Barskey, A.E., Shah, P.P., Schrag, S., Whitney, C.G., Arduino, M.J., Reddy, S.C.,
686 Kunz, J.M., Hunter, C.M., Raphael, B.H., Cooley, L.A., 2017. Vital Signs: Health
687 Care–Associated Legionnaires’ Disease Surveillance Data from 20 States and a Large
688 Metropolitan Area — United States, 2015. *MMWR Morb. Mortal. Wkly. Rep.* 66,
689 584–589. <https://doi.org/10.15585/mmwr.mm6622e1>

690 Souiri, M., Blel, N., Sboui, D., Mhamdi, L., Epalle, T., Mzoughi, R., Riffard, S., Othmane,
691 A., 2014. AFM, CLSM and EIS characterization of the immobilization of antibodies
692 on indium–tin oxide electrode and their capture of *Legionella pneumophila*. *Talanta*
693 118, 224–230. <https://doi.org/10.1016/j.talanta.2013.09.049>

694 Vashist, S.K., 2012. Comparison of 1-Ethyl-3-(3-Dimethylaminopropyl) Carbodiimide Based
695 Strategies to Crosslink Antibodies on Amine-Functionalized Platforms for
696 Immunodiagnostic Applications. *Diagnostics* 2, 23–33.
697 <https://doi.org/10.3390/diagnostics2030023>

698 Vashist, S.K., Dixit, C.K., MacCraith, B.D., O’Kennedy, R., 2011. Effect of antibody
699 immobilization strategies on the analytical performance of a surface plasmon
700 resonance-based immunoassay. *The Analyst* 136, 4431.
701 <https://doi.org/10.1039/c1an15325k>

702 Vashist, S.K., Marion Schneider, E., Lam, E., Hrapovic, S., Luong, J.H.T., 2015. One-step
703 antibody immobilization-based rapid and highly-sensitive sandwich ELISA procedure
704 for potential in vitro diagnostics. *Sci. Rep.* 4. <https://doi.org/10.1038/srep04407>

705 Walker, J., 2018. The influence of climate change on waterborne disease and *Legionella* : a
706 review. *Perspect. Public Health* 138, 282–286.
707 <https://doi.org/10.1177/1757913918791198>

708 Yun, Y., Bange, A., Heineman, W.R., Halsall, H.B., Shanov, V.N., Dong, Z., Pixley, S.,
709 Behbehani, M., Jazieh, A., Tu, Y., 2007. A nanotube array immunosensor for direct
710 electrochemical detection of antigen–antibody binding. *Sens. Actuators B Chem.* 123,
711 177–182. <https://doi.org/10.1016/j.snb.2006.08.014>

712 Zhang, C., Lou, J., Tu, W., Bao, J., Dai, Z., 2015. Ultrasensitive electrochemical biosensing
713 for DNA using quantum dots combined with restriction endonuclease. *The Analyst*
714 140, 506–511. <https://doi.org/10.1039/C4AN01284D>
715 Zhang, X., Shen, G., Sun, S., Shen, Y., Zhang, C., Xiao, A., 2014. Direct immobilization of
716 antibodies on dialdehyde cellulose film for convenient construction of an
717 electrochemical immunosensor. *Sens. Actuators B Chem.* 200, 304–309.
718 <https://doi.org/10.1016/j.snb.2014.04.030>
719